Control of apical membrane chloride permeability in the renal A6 cell line by nucleotides

U. Banderali, E. Brochiero, S. Lindenthal, C. Raschi, S. Bogliolo and J. Ehrenfeld

Laboratoire de Physiologie des Membranes cellulaires (laboratoire Jean Maetz), Université de Nice Sophia-Antipolis, ERS 1253 CNRS, Villefranche-sur-mer, France

(Received 11 March 1999; accepted after revision 17 June 1999)

1. The effect of extracellular nucleotides applied on the apical side of polarised A6 cells grown on permeant filters was investigated by measuring the changes in (i) the ^{36}Cl efflux through the apical membranes, (ii) the intracellular chloride concentrations (aCl_i, measured with *N*-(6-methoxyquinolyl) acetoethyl ester, MQAE), (iii) I_{Cl}, the short-circuit current in the absence of Na^+ transport and (iv) the characteristics of the apical chloride channels using a patch-clamp approach.

2. ATP or UTP (0·1–500 μM) transiently stimulated I_{Cl}. The sequence of purinergic agonist potencies was UTP = ATP > ADP $\gg$ the P2X-selective agonist β,γ-methylene ATP = the P2Y-selective agonist 2-methylthioATP. Suramin (100 μM) as the P2Y antagonist Reactive Blue 2 (10 μM) had no effect on the UTP (or ATP)-stimulated current. These findings are consistent with the presence of $P2Y_2$-like receptors located on the apical membranes of A6 cells. Apical application of adenosine also transiently increased I_{Cl}. This effect was blocked by theophylline while the UTP-stimulated I_{Cl} was not. The existence of a second receptor, of the P1 type is proposed.

3. ATP (or UTP)-stimulated I_{Cl} was blocked by apical application of 200 μM *N*-phenylanthranilic acid (DPC) or 100 μM niflumic acid while 100 μM glibenclamide was ineffective.

4. Ionomycin and thapsigargin both transiently stimulated I_{Cl}; the nucleotide stimulation of I_{Cl} was not suppressed by pre-treatment with these agents. Chlorpromazin (50 μM), a Ca^{2+}–calmodulin inhibitor strongly inhibited the stimulation of I_{Cl} induced either by apical UTP or by ionomycin application. BAPTA-AM pre-treatment of A6 cells blocked the UTP-stimulated I_{Cl}. Niflumic acid also blocked the ionomycin stimulated I_{Cl}.

5. A fourfold increase in ^{36}Cl effluxes through the apical membranes was observed after ATP or UTP application. These increases of the apical chloride permeability could also be observed when following aCl_i changes. Apical application of DPC (1 mM) or 5-nitro-2(3-phenylpropylamino)benzoic acid (NPPB; 500 μM) produced an incomplete inhibition of ^{36}Cl effluxes through the apical membranes in ATP-stimulated and in untreated monolayers.

6. In single channel patch-clamp experiments, an apical chloride channel with a unitary single channel conductance of 7·3 $\pm$ 0·6 pS ($n = 12$) was usually observed. ATP application induced the activation of one or more of these channels within a few minutes.

7. These results indicate that multiple purinergic receptor subtypes are present in the apical membranes of A6 cells and that nucleotides can act as modulators of Cl^- secretion in renal cells.

The cultured amphibian renal A6 cell line forms well-differentiated monolayers and has been used as a model for Na^+ and Cl^- transport in epithelia of high resistance. Under resting conditions, the short-circuit current corresponds to an amiloride-sensitive sodium transport under hormonal regulation (Perkins & Handler, 1981; Sariban-Sohraby *et al.* 1983). In addition, on stimulation with antidiuretic hormones or prostaglandin E_2 (PGE_2), a significant chloride secretion has also been reported and is reflected by an early and rapid development of a transepithelial short-circuit current, I_{Cl} (Chalfant *et al.* 1993; Verrey, 1994). Chloride secretion after hormonal stimulation was considered to be due to a two-step process involving a Na^+–K^+–$2Cl^-$ cotransporter in the basolateral membranes (Yanase & Handler, 1986; Fan *et al.* 1992; Brocchiero *et al.* 1995*a*) and an electrodiffusional pathway on the apical membranes mediated by the stimulation of various classes of chloride channel (3 and 8 pS unit conductances) as revealed by patch-clamp experiments

(Marunaka & Eaton, 1990*a*,*b*; Marunaka, 1993; Marunaka & Tohda, 1993).

In various types of epithelia, Cl^- secretion has also been shown to be stimulated by extracellular nucleotides and in particular by ATP (Clarke & Boucher, 1992; Dho *et al.* 1992; Zegarra-Moran *et al.* 1995). This effect on ion transport is one of a number of biological responses elicited by the binding of nucleotides onto purinergic receptors distributed on the cell surface. In A6 cells, extracellular ATP was found to activate K^+ and Cl^- currents (Middleton *et al.* 1993; Nilius *et al.* 1995) simultaneously with Ca_i^{2+} release (Middleton *et al.* 1993; Nilius *et al.* 1995). Mori *et al.* (1996) also found an elevation of Ca_i^{2+} after adenine nucleotide application and a stimulation of calcium-dependent cation channels, this latter effect implicating P2Y receptors. In all studies, A6 cells were seeded on glass coverslips or plastic culture wells, an experimental procedure which facilitates whole-cell patch-clamp studies such as fura-2 fluorescence measurements but which does not allow the establishment of a polarised and functional epithelial cell monolayer.

The aim of the present study was to investigate, in polarised A6 cells grown on permeant filters, the effect of extracellular nucleotides applied to the apical side of the monolayer on the mechanism of chloride secretion. We wished to identify the type of nucleotide receptor(s) involved and the effects on the nucleotides on the different chloride channels reported in A6 apical cell membranes. For this, kinetic experiments (^{36}Cl effluxes through the apical membranes and intracellular chloride concentrations (aCl_i) measurements) as well as electrophysiological techniques (I_{Cl} and patch-clamp experiments) were performed. Special attention was given to the role of intracellular calcium (Ca_i^{2+}) as a signal transduction pathway.

We showed that multiple nucleotide receptors located on the apical surface of the cell monolayer may control the chloride secretion in this model renal cell line.

METHODS

Cell culture

A6, a renal cell line from *Xenopus laevis* was a gift from Dr Rossier (Lausanne, Switzerland). It had originally been obtained from the American Tissue Type Collection and was subsequently cloned (clone A6-2F3) by limiting dilution (Verrey *et al.* 1987). Cells were grown between passages 88 and 98 at 28 °C in a humidified atmosphere of 5% CO_2 in air. The amphibian cell medium (AM) (Handler *et al.* 1979) was supplemented three times weekly with 10% fetal calf serum (IBF, France) for cell nourishment and with penicillin (0·06 mg ml^{-1}) and streptomycin (0·13 mg ml^{-1}). The osmolarity of AM was measured using a vapour pressure osmometer (Model 5500, Wescor, Logan, UT, USA) and was found to be 247 mosmol l^{-1}.

Cells were seeded onto transparent collagen-treated membranes (Transwell, 0·45 μm pore, Costar, MA, USA) at a seeding density of 2×10^6 cells per well (4·9 cm^2). Cell monolayers were then fed for 5–10 days with the amphibian medium (serum-free) supplemented with 2% ultroser-G (Gibco–IBF, USA–France) in order to increase their Na^+ transport capacity.

^{36}Cl efflux measurements through the apical membranes

The cell monolayer was incubated for 15 min in a Ringer solution containing 5 μl ml^{-1} ^{36}Cl (1 mCi ml^{-1}, ICN, France). After three rapid washes of both sides of the monolayer, ^{36}Cl effluxes were measured during two successive 5 min periods, by sampling the solutions in contact with the apical and serosal sides of the monolayer. At the end of the experiment, cells were digested in a 10% SDS solution and placed, as were the experimental samples, in counting vials supplemented with 10 ml ACS (Amersham, USA) for counting in a liquid scintillation counter (Packard Instruments, USA). ^{36}Cl effluxes were expressed as a fraction of the intracellular value at the beginning of the measurement period. The serosal solution contained 50 μM NPPB and 1 mM furosemide in order to reduce ^{36}Cl effluxes through the basolateral membranes. The half-time of cell ^{36}Cl effluxes under control conditions was about 5–7 min.

Intracellular chloride measurements

The method of measuring intracellular chloride concentration (aCl_i) using *N*-(6-methoxyquinolyl) acetoethyl ester (MQAE, Molecular Probes, Eugene, OR, USA) as a Cl^- probe was similar to that described previously (Crowe *et al.* 1995; Brochiero *et al.* 1995*a*). The dye-loading procedure did not affect the Na^+ ion transport since monolayers loaded with MQAE presented short-circuit currents of 16·0 ± 1·8 μA cm^{-2} and transepithelial potentials of 50 ± 4 mV ($n = 26$), values similar to those previously found (Ehrenfeld *et al.* 1994) and which were completely blocked by addition of amiloride (50 μM) to the apical bathing solution. In brief, A6 monolayers were loaded overnight in amphibian cell culture medium containing 5 mM MQAE at 28 °C, in a CO_2 incubator. After several rapid washes, the filter and monolayer were cut off the support and mounted in an adapted Ussing chamber placed in the sample compartment of a spectrophotometer system (PTI Deltascan, NJ, USA). Both sides of the monolayer were continuously perfused with Ringer solutions (see below) at a constant rate of 3 ml min^{-1} using a peristaltic pump (Ismatec, Germany). The excitation light was set at 360 nm and the emission monitored at 450 nm (6 nm band pass). A maximal intensity of fluorescence (F_o) was observed and determined for each monolayer by perfusion with a Cl^--free solution (for composition see below) on both sides of the monolayer. The fluorescence intensity was measured every second and plotted graphically. At the end of an experiment the monolayer was perfused with KSCN (120 mM) solution (buffered with 10 mM Hepes–KOH, pH 7·2) which quenched MQAE fluorescence by more than 90%. For data analysis, the KSCN-quenched fluorescence value was substracted from the fluorescence measured experimentally. Cellular autofluorescence was also measured in epithelia not exposed to MQAE and found not to exceed 5% of the fluorescence from dye-loaded cells. This value was subtracted before intracellular chloride (aCl_i) determination. To calculate aCl_i, a calibration curve was established (see Brochiero *et al.* 1995*a*).

Intracellular calcium measurements

Experiments were performed as previously reported (Brochiero *et al.* 1995*b*) with intact monolayers using the acetoxymethyl ester form of fura-2 (fura-2 AM; Molecular Probes) as a probe of intracellular calcium activity. In brief, cell monolayers were loaded with 10 μM fura-2 AM at 28 °C for 90 min, in a CO_2 incubator. In preliminary experiments we determined that a 90 min fura-2 loading was necessary to improve the signal/background ratio. After several rapid washings, the filter supporting the monolayer was removed from the Transwell, mounted in an adapted Ussing chamber placed in the sample compartment of a spectrophotometer system (PTI, Deltascan) and perfused with Ringer solutions. An

equilibration period (stability of the 340/380 ratio) of 5–10 min was waited before starting the experiment. The excitation light was set to alternate between 340 and 380 nm (4 nm band pass) at a rate of 100 Hz and the emission was monitored at 505 nm (6 nm band pass). The fluorescence intensity ratio (I_{340}/I_{380}) was measured every second and plotted graphically. To calculate the calcium concentration, the Grynkiewicz equation was used, with a K_d value of 224 nM as reported by Grynkiewicz *et al.* (1985). At the end of each experiment the fluorescence ratios in the absence and presence of saturating Ca^{2+} (R_{min} and R_{max}) were determined as previously described (Brochiero *et al.* 1995*b*).

Electrical measurements (transepithelial potential, short-circuit current and resistance of monolayers) were carried out in a home-made modified Ussing chamber designed to fit the Transwell. The volumes of apical and basolateral bathing solutions were 2 ml and 2·5 ml, respectively, and the solutions could be changed without interruption of measurements. The spontaneous transepithelial potential (PD) was measured through Agar–KCl salt bridges and was clamped at 0 V, through platinum electrodes, using an automatic voltage clamp (Model VC 600, Physiological Instruments, Houston, TX, USA). The short-circuit current (I_{SC}) and additional pulses (10 mV, 1 s duration every 60 s) to measure the monolayer resistance (R) were continuously recorded on a chart paper recorder (SEFRAM, France).

Patch-clamp experiments

Patch-clamp experiments were made on the apical domains of confluent monolayers of A6 cells. The patch electrodes were obtained by a double pulling of glass capillaries (Vitrex, Denmark) on a Narishige (Tokyo, Japan) vertical puller and their resistance was 8–10 MΩ. The pipette solutions contained (mM): NMDG-Cl, 145; $MgCl_2$, 3; Hepes, 5; EGTA, 1 (pH 7·4). The patch-clamp amplifier was a Biologic RK300 (Claix, France) and the signal was recorded on magnetic tape with a betamax video recorder (Sony) after conversion to a video signal by a Biologic PCM converter. The signal was then analysed using a Compaq ProLinea 4/50 microcomputer with Cambridge Electronic Design (Cambridge, UK) software and A/D interface.

Single channel data analysis: estimation of the number of channels in a patch

Two different methods were used to estimate the number of channels in the patches in which several active channels were observed at the same time. In the recordings from cells in control conditions (i.e. before stimulation by luminal ATP), the number of channels in the patch was evaluated using the N_T (number of transitions) estimator, as recently described by Denicourt *et al.* (1996). This estimator can be applied to the recordings containing several identical and independent channels in a stationary situation. It consists of counting the number of transitions of the signal between two adjacent current levels, each level corresponding to a number of simultaneously open channels. In a multiple channel recording, the number of channels N can be deduced from the following equation:

$$T_{r,r+}/T_{r+1,r+2} = (N-r)/(N-1-r),$$

where $T_{r,r+1}$ is the number of transitions per second from the current level corresponding to r open channels to the one corresponding to $r+1$ open channels ($0 \leqslant r \leqslant N-1$). Two important conditions must be met for a successful application of this esimator: (a) the probability of observing r simultaneous open channels must obey the binomial distribution and (b) the ensemble of channels must be in a stationary situation. The stationarity of the multiple channel recordings was tested with the method described by Denicourt *et al.* (1996): the mean current $\bar{I}$ was measured over M independent 1 s segments of the signal, the stochastic variable A was then defined as follows:

$$A = \sum_{j=1}^{M-1} \sum_{k=j}^{M} a_{jk},$$

where: $a_{jk} = 1$ if $\bar{I}_k > \bar{I}_j$; $a_{jk} = 0$ otherwise and $1 \leqslant j \leqslant M-1$; $j \leqslant k \leqslant M$.

The signal was considered stationary when the experimental value of A fell within the 95% confidence interval of the theoretical distribution of the stochastic variable.

Conditions (a) and (b) were fulfilled only in the signal recordings before the addition of ATP to the luminal solution. Stimulation of chloride secretion by ATP increased the activity of apical chloride channels. In the patch-clamp experiments, this stimulation appeared as a transient rise in the number of active channels and the signal obviously was no longer stationary. Therefore, under these conditions, the number of channels in the patch (N) was evaluated using the MAX estimator (Horn, 1991): k_{MAX} = the maximum number of simultaneously open channels and $N \geqslant k_{MAX}$.

Statistics

Data variability is expressed as S.E.M. Student's t test was used for estimating the significance of differences between paired mean data.

Drugs and Ringer solution compositions

ATP and UTP, ADP, β,γ-methylene ATP, 2-methylthioATP, suramin, Reactive Blue 2 and BAPTA AM were purchased from Sigma Chemical Co. (St Louis, MO, USA); amiloride was from Interchim (France), *N*-phenylanthranilic acid (DPC) was from Fluka (Switzerland) and 5-nitro-2(3-phenylpropylamino)benzoic acid (NPPB) was a gift of Dr Greger (Freiburg, Germany).

The perfusing solutions had the following compositions. Chloride-containing medium (mM): NaCl, 83; $NaHCO_3$, 24; KCl, 2·5; $CaCl_2$, 2; $MgSO_4$, 2; Na_2HPO_4, 3·2; KH_2PO_4, 1·2; glucose, 11; Hepes, 5, pH 7·4 after bubbling with 5% CO_2. Chloride-free medium (mM): $NaNO_3$, 83; $NaHCO_3$, 24; KNO_3, 2·5; $CaNO_3$, 2; $MgSO_4$, 2; Na_2HPO_4, 3·2; KH_2PO_4, 1·2; glucose, 11; Hepes 5; pH 7·4 after bubbling with 5% CO_2.

RESULTS

Nucleotide-induced increase in apical chloride permeability

The effects of apical application of nucleotides on I_{SC} were investigated in the absence of sodium transport (i.e. in the presence of amiloride). This experimental procedure was previously used to study the chloride current (I_{Cl}) which develops after AVT or PGE_2 application in A6 cells (Chalfant *et al.* 1993; Verrey, 1994). The electrophysiological characteristics of the untreated A6 cell monolayers, plated for 8–10 days on permeant filters were as follows: short-circuit current (I_{SC}), transepithelial voltage (V_t) and transepithelial conductance (G_t) were 21·8 ± 2·1 μA cm^{-2}, 72·8 ± 3·8 mV and 0·30 ± 0·03 mS, respectively ($n = 13$). Application of 50 μM amiloride reduced these values to 1·4 ± 0·4 μA cm^{-2} (I_{SC}), 14·1 ± 2·4 mV (V_t) and 0·07 ± 0·01 mS (G_t), as expected with Na^+ transport blockade.

Addition of 300 μM ATP to the apical solution elicited a rapid transient increase in I_{Cl} and G_t (Fig. 1*A*). A maximum

current ($6{\cdot}2 \pm 1{\cdot}4$ μA cm^{-2}, $n = 13$) was reached at 82 ± 6 s after ATP application which was followed by a progressive I_{Cl} decline ($2{\cdot}6 \pm 0{\cdot}6$ μA cm^{-2} at $18{\cdot}0 \pm 1{\cdot}5$ min). The transepithelial conductance followed a similar pattern ($G_t = 0{\cdot}36 \pm 0{\cdot}05$ mS for the peak and $0{\cdot}13 \pm 0{\cdot}03$ mS after 18 min ATP application) while V_t was only slightly affected ($15 \pm 1{\cdot}6$ mV and $18{\cdot}8 \pm 2{\cdot}1$ mV for the same times of measurement after ATP application). Apical application of 200 μM DPC, a chloride channel blocker, blocked the ATP response (Fig. 1) supporting the assumption that I_{SC} was due to the nucleotide stimulation of a serosal-to-mucosal chloride transport (the ATP-stimulated I_{Cl} maxima were $4{\cdot}3 \pm 0{\cdot}4$ and $1{\cdot}0 \pm 0{\cdot}1$ μA cm^{-2} in the absence and presence of DPC, respectively, $n = 4$). Glibenclamide (100 μM), which also inhibits Cl^- channels (Sheppard & Welsh, 1993; Rabe *et al.* 1995) was ineffective (the ATP-stimulated currents were $7{\cdot}2 \pm 2{\cdot}8$ and $8{\cdot}9 \pm 3{\cdot}2$ μA cm^{-2} in the absence and presence of glibenclamide, respectively, $n = 4$). A similar I_{Cl} stimulation was found with an apical application of 300 μM UTP (Fig. 2*A*). Serosal application of UTP also stimulated I_{Cl}, indicating the presence of receptors on the basolateral membranes also. The apical UTP-induced I_{Cl} was almost completely inhibited by DPC application (Fig. 2*B*; the UTP-stimulated I_{Cl} maxima were $6{\cdot}5 \pm 1{\cdot}8$ and $0{\cdot}4 \pm 0{\cdot}2$ μA cm^{-2} in the absence and presence of DPC, respectively, $n = 4$). Apical application of 100 μM niflumic acid, another known Cl^- channel blocker, almost completely inhibited the UTP-stimulated I_{Cl} (100 μM UTP-stimulated I_{Cl} maxima were $4{\cdot}4 \pm 0{\cdot}5$ and $0{\cdot}5 \pm 0{\cdot}2$ μA cm^{-2} in the absence and presence of niflumic acid, respectively, $n = 3$). Application of 500 μM DIDS induced a smaller inhibition than niflumic acid (100 μM UTP-stimulated I_{Cl} maxima were $3{\cdot}5 \pm 0{\cdot}4$ and $2{\cdot}0 \pm 0{\cdot}5$ μA cm^{-2} in the absence and presence of DIDS, respectively, $n = 5$).

In a second series of experiments, we followed the changes in the Cl^- transport rates across the apical cell membranes by measuring the MQAE fluorescence as an index of the intracellular Cl^- concentration (aCl_i). For this, Cl^- transport rates across apical A6 cell membranes were measured by following the initial (20 s) changes in aCl_i (expressed in arbitrary slope changes in F/F_o, 10^{-3} s^{-1}) or maximal aCl_i variations (in mM) after substitution of chloride in the medium by nitrate. As already reported (Brochiero *et al.* 1995*a*), untreated monolayers exhibited a low apical Cl^- permeability which was found to be much lower than that of the basolateral membranes in 92% of the 124 monolayers tested. Mean aCl_i variations were $-4{\cdot}7 \pm 0{\cdot}5$ and $4{\cdot}9 \pm 0{\cdot}5$ mM for apical Cl^- depletion (NO_3^- substitution) and repletion, respectively, while the mean aCl_i variations on the basolateral side were $-21{\cdot}5 \pm 0{\cdot}95$ and $23{\cdot}9 \pm 1{\cdot}01$ mM, respectively ($n = 124$). The effect of ATP application was investigated by following the aCl_i variations induced by apical Cl^- substitution. The substitution was performed

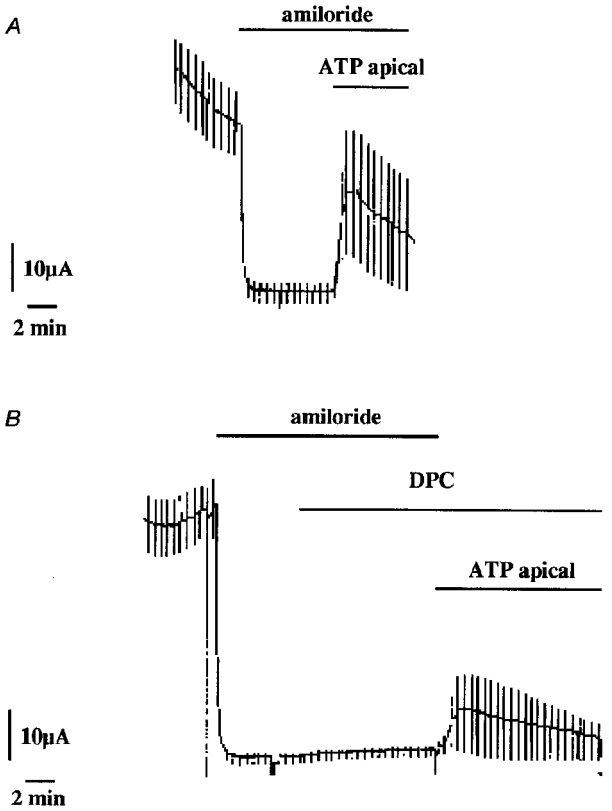

Figure 1. The effect of ATP application on the short-circuit current in A6 cell monolayers
ATP (300 μM) was applied on the apical side in the presence of 50 μM amiloride in order to block sodium transport (*A*). The ATP-stimulated short-circuit current was inhibited by the presence of 200 μM DPC in to the apical solution (*B*). The current is given in μA for a filter surface area of 4·9 cm^2.

Table 1. Effects of 300 μM ATP on Cl^- transport across the apical membranes

	aCl_i			F/F_o		
	Control (mM)	ATP (mM)	Difference (mM)	Control (10^{-3} s^{-1})	ATP (10^{-3} s^{-1})	Difference (10^{-3} s^{-1})
A. Nucleotide added to the apical side only						
Apical ATP ($n = 8$)						
$Cl \rightarrow NO_3$	$-0{\cdot}4 \pm 0{\cdot}3$	$-7{\cdot}5 \pm 1{\cdot}5$	$-7{\cdot}1 \pm 1{\cdot}6$****	$0{\cdot}02 \pm 0{\cdot}01$	$0{\cdot}51 \pm 0{\cdot}13$	$0{\cdot}49 \pm 0{\cdot}14$***
$NO_3 \rightarrow Cl$	$+0{\cdot}5 \pm 0{\cdot}3$	$+9{\cdot}0 \pm 1{\cdot}9$	$+8{\cdot}5 \pm 1{\cdot}9$*****	$0{\cdot}02 \pm 0{\cdot}01$	$0{\cdot}60 \pm 0{\cdot}15$	$0{\cdot}58 \pm 0{\cdot}15$***
B. Nucleotide applied first to the basolateral side then to the apical side						
Basolateral ATP ($n = 5$)						
$Cl \rightarrow NO_3$	$-1{\cdot}4 \pm 0{\cdot}2$	$-4{\cdot}8 \pm 1{\cdot}1$	$-3{\cdot}4 \pm 1{\cdot}0$****	$0{\cdot}20 \pm 0{\cdot}12$	$0{\cdot}40 \pm 0{\cdot}13$	$0{\cdot}20 \pm 0{\cdot}14^{n.s.}$
$NO_3 \rightarrow Cl$	$+2{\cdot}2 \pm 0{\cdot}5$	$+5{\cdot}2 \pm 1{\cdot}1$	$+3{\cdot}0 \pm 1{\cdot}1$****	$0{\cdot}18 \pm 0{\cdot}04$	$0{\cdot}37 \pm 0{\cdot}13$	$0{\cdot}19 \pm 0{\cdot}15$*
Apical ATP ($n = 5$)						
$Cl \rightarrow NO_3$	$-1{\cdot}4 \pm 0{\cdot}2$	$-7{\cdot}0 \pm 1{\cdot}8$	$-5{\cdot}6 \pm 1{\cdot}6$****	$0{\cdot}20 \pm 0{\cdot}12$	$0{\cdot}71 \pm 0{\cdot}23$	$0{\cdot}51 \pm 0{\cdot}15$**
$NO_3 \rightarrow Cl$	$+2{\cdot}2 \pm 0{\cdot}5$	$+7{\cdot}2 \pm 1{\cdot}9$	$5{\cdot}0 \pm 1{\cdot}8$****	$0{\cdot}18 \pm 0{\cdot}04$	$0{\cdot}48 \pm 0{\cdot}13$	$0{\cdot}30 \pm 0{\cdot}18$**

$[Cl^-]_i$ changes and the rates of chloride transport (F/F_o, 10^{-3} s^{-1}) were followed when perfusing the apical side of the A6 cell monolayer with Cl^--containing Ringer solution being replaced by NO_3^--containing Ringer solution ($Cl \rightarrow NO_3$) or *vice versa* ($NO_3 \rightarrow Cl$). ATP was added to the solution bathing the apical side of the A6 cell monolayer 1 min before chloride substitution (A). In B, the ATP effect was followed when adding the nucleotide to the basolateral side then to the apical side (see Fig. 3*B*). Significance levels: n.s., not significant; * $P < 0{\cdot}1$; ** $P < 0{\cdot}05$; *** $P < 0{\cdot}010$; **** $P < 0{\cdot}005$.

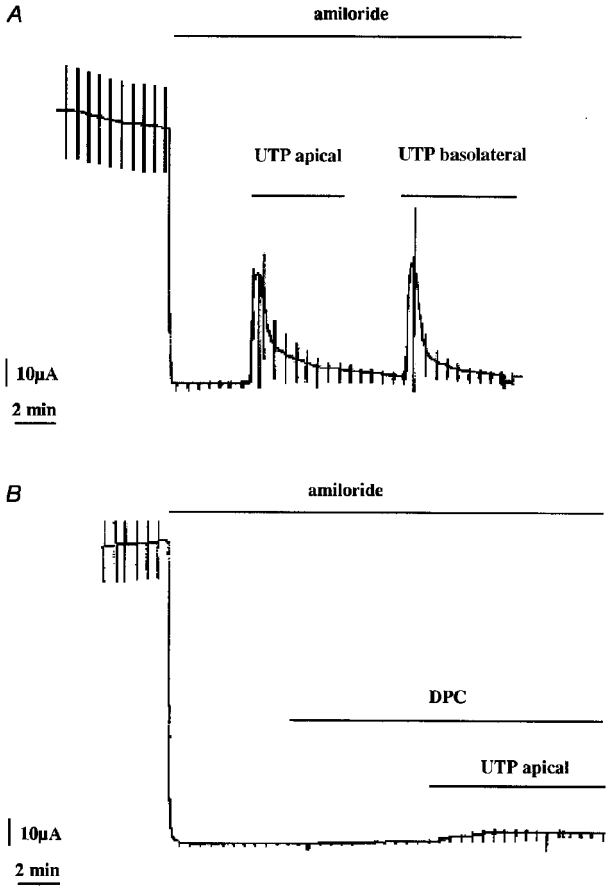

Figure 2. The effect of UTP application on the short-circuit current in A6 cell monolayers
UTP (300 μM) was applied on the apical side in the presence of 50 μM amiloride in order to block sodium transport (*A*). The UTP-stimulated short-circuit current was inhibited by the presence of 200 μM DPC in the apical solution (*B*).

twice on the same monolayer, a control period preceding the experimental one. Apical ATP application (300 μM) stimulated the apical chloride permeability considerably as seen in the $a\mathrm{Cl_i}$ changes and the slope changes in $a\mathrm{Cl_i}$ (F/F_o, 10^{-3} s^{-1}) following anion subsitution (Table 1A). Figure 3*A* illustrates the effects of ATP stimulation of a monolayer presenting a very low apical chloride permeability in control conditions. Basolateral ATP application (300 μM) also stimulated the apical chloride permeability (Fig. 3*B* and Table 1B) but the effect was less than that observed with the same nucleotide concentration applied to the apical side of the monolayer (compare ATP responses in Table 1 and Fig. 3*B*). Note that the initial basolateral ATP application did not prevent the apical ATP response. UTP (300 μM) produced similar effects to ATP added to either the apical or serosal side of the monolayer (Fig. 3*C*).

The stimulatory effect of apical ATP application on chloride transport through the apical membranes was directly confirmed by ^{36}Cl efflux measurements. A6 cell monolayers were loaded with ^{36}Cl and ^{36}Cl effluxes through both membranes (apical and basolateral) were then followed in the absence and presence of apical ATP (300 μM). As evident from Fig. 4, in non-treated monolayers, ^{36}Cl effluxes were much higher through the basolateral than through the apical membrane (in agreement with $a\mathrm{Cl_i}$ changes observed after apical or basolateral chloride substitution, see above). However, when ^{36}Cl effluxes were measured in the presence of ATP (apical side), a fourfold increase in ^{36}Cl effluxes through the apical membranes was observed (Fig. 4*A*). Consequently, the Cl^- effluxes through the basolateral membranes were reduced since the ^{36}Cl-specific radioactivity in the cell decreased. Apical application of DPC (1 mM) or

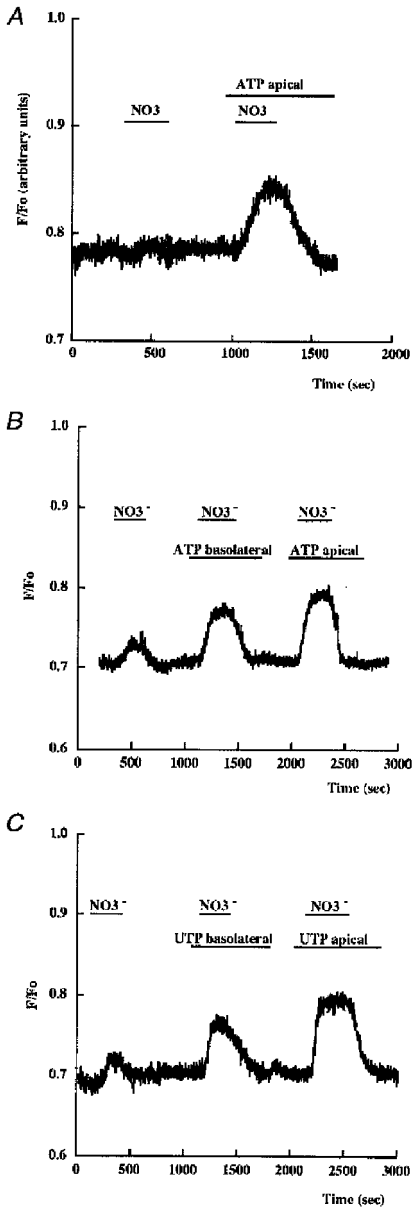

Figure 3. Effects of ATP and UTP on apical Cl^- permeability ($a\mathrm{Cl_i}$ changes) in A6 cells

Changes in the F/F_o ratio of MQAE fluoresence were followed after substitution of nitrate for chloride in the apical perfusing medium. A typical experiment is shown representing F/F_o changes observed in the absence or presence of 300 μM ATP on the apical side of a monolayer presenting a very low Cl^- permeability before nucleotide addition (*A*). In *B* the effect of ATP applied first to the basolateral then to the apical side is reported for a monolayer presenting a low Cl^- permeability before nucleotide addition. The effect of UTP is shown in *C*.

NPPB (500 μM) produced a partial inhibition of ^{36}Cl effluxes through the apical membranes in ATP-stimulated (Fig. 4*C*) and untreated monolayers (Fig. 4*B*).

Characterisation of the Cl^- channel involved after nucleotide application

In single channel patch-clamp experiments patch pipettes were applied on the apical membranes of polarised confluent A6 cells monolayers. The cells were initially placed in Ringer solution. After giga-seal formation, 300 μM ATP was added to the solution bathing the apical membranes, external to the patch pipette.

In a series of 50 successful experiments, activation of chloride channels in response to ATP occurred in twelve experiments. The *I–V* relationship of these channels (Fig. 5*A*), recorded in the cell-attached configuration, was linear and the unitary single channel conductance was $7{\cdot}3 \pm 0{\cdot}6$ pS ($n = 12$).

In eight of 12 recordings no chloride channels were observed in control conditions but addition of ATP induced the activation of one or more channels within a few minutes. The delay between ATP addition and channel activation varied from 1 to 5 min with an average time of $2{\cdot}6 \pm 0{\cdot}5$ min. In the other four recordings, one or more 7·3 pS channels were already present in control conditions and the addition of the nucleotide transiently enhanced their activity. This was revealed by an increase in the number of current levels in the recording (indicating simultaneous openings of a larger number of channels) which reached a maximum $1{\cdot}7 \pm 0{\cdot}7$ min after addition of ATP and then decreased to lower values (Fig. 6). This kind of pattern could result either from an actual increase in the number of active channels in the patch or from an increase in the open probability of a constant number of channels. In order to clarify this point, an estimation of the number of active channels in the

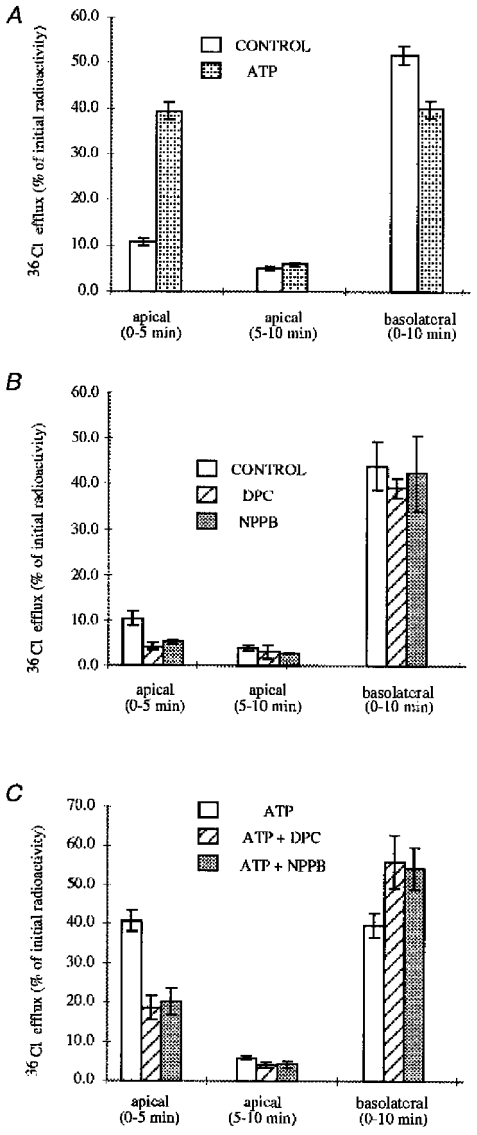

Figure 4. ATP stimulation of ^{36}Cl effluxes through the apical membranes in A6 cells

Effects of DPC and NPPB. In untreated monolayers, ^{36}Cl effluxes were much higher through the basolateral membrane than through the apical membrane. Apical application of 300 μM ATP stimulated ^{36}Cl effluxes through these membranes. As a consequence, the Cl^- effluxes through the basolateral membranes were reduced since the ^{36}Cl-specific radioactivity of the cell decreased (*A*). Apical applicationof DPC (1 mM) or NPPB (500 μM) produced a partial inhibition of ^{36}Cl effluxes through the applical membranes in ATP-stimulated (*C*) or in untreated monolayers (*B*).

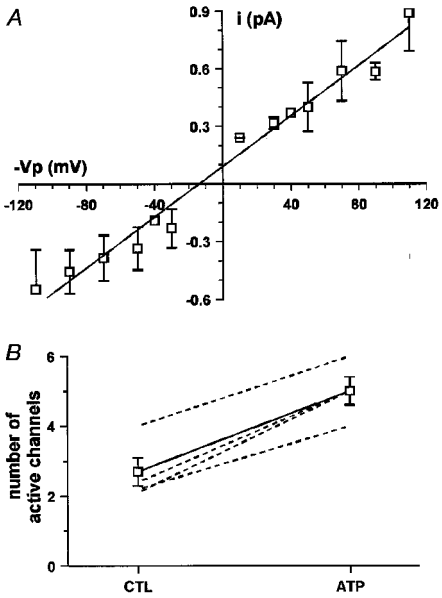

Figure 5. ATP stimulation of apical chloride channels and their I–V relationship

A, current–voltage relationship of the chloride channel stimulated by luminal ATP. The unitary conductance of the channel was 7·3 pS (V_p, pipette potential). *B*, luminal ATP increases the number of active channels. The number of active channels in the patch was evaluated using the N_T estimator in the recording under control conditions (CTL) and the MAX estimator in the recording after ATP addition. Dashed lines are results from single experiments and the continuous line is the average.

patches (N) was performed both in control conditions and after ATP stimulation of the cell. For this analysis, two different estimators were used: the N_T estimator in the control recordings (i.e. when the channels were stationary and the distribution of current levels obeyed the binomial law) and the MAX estimator after addition of ATP (see materials and methods). It is important to note that MAX is more precise when N is small ($N < 4$) and generally underestimates the actual number of channels in a patch (Horn, 1991). In the four different experiments the number of active channels in control conditions varied between two and four but increased to values between four and six after ATP addition, as shown in Fig. 5*B*.

Analysis of the kinetic behaviour of the channels showed that both the open and the closed dwell time distributions could be fitted by double exponential functions with the following time constants (where o indicates open and c closed): $\tau_{o1} = 24$ ms and $\tau_{o2} = 170$ ms (number of events, 1166); $\tau_{c1} = 161$ ms and $\tau_{c2} = 804$ ms (number of events, 524).

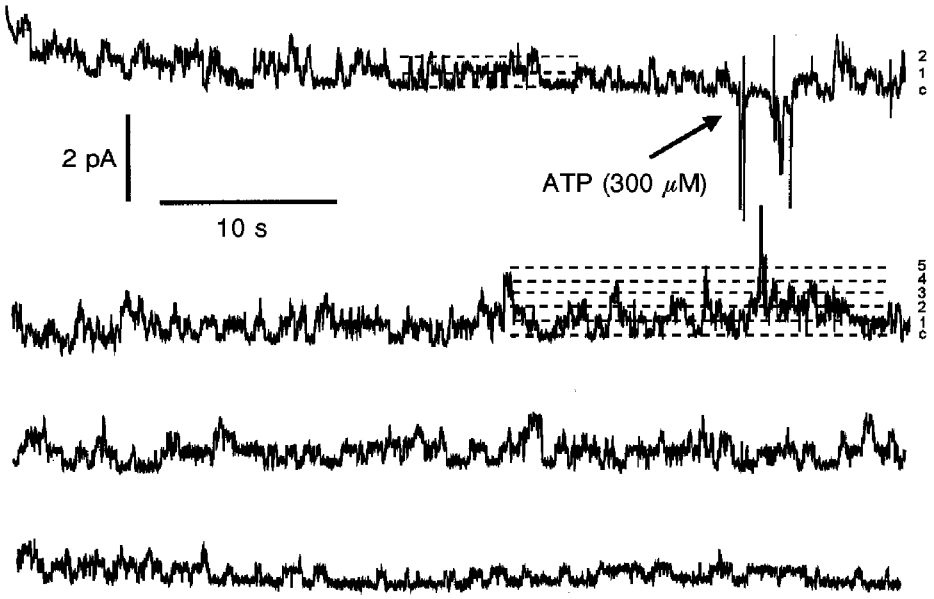

Figure 6. Stimulation of apical chloride channel activity by luminal ATP

Recording showing apical chloride channel activity before and after addition of 300 μM ATP to the luminal solution. In control conditions, the signal revealed the activity of two channels. In contrast, up to five different channels could open simultaneously 1 min after addition of ATP. The dashed lines represent the current levels corresponding to all channels closed and up to five channels open at the same time.

Identification of the apical nucleotide receptor subtype implicated in the chloride secretion stimulation

The sequence of purinergic agonist potencies for activating the chloride currents was investigated in order to define the type of nucleotide receptor(s) involved.

The peak I_{SC}–concentration relationships for the currents activated by apical nucleotide application is illustrated in Fig. 7. From the half-maximal concentration (EC_{50}) values, the order of agonist potency for activating the currents was UTP ($2{\cdot}5 \pm 1{\cdot}4$ μM) = ATP ($3{\cdot}2 \pm 0{\cdot}12$ μM) > ADP ($46{\cdot}0 \pm 25{\cdot}9$ μM) ≫ the P2X-selective agonist β,γ-methylene ATP = the P2Y-selective agonist 2-methylthioATP. The absence of P2X receptors suggested by the poor I_{Cl} sensitivity to the P2X-selective agonist β,γ-methylene ATP was confirmed by the lack of inhibitory effect of 100 μM suramin application on the UTP-stimulated current (10 μM UTP, maximal I_{Cl} was $5{\cdot}8 \pm 0{\cdot}5$ and $8{\cdot}1 \pm 1{\cdot}2$ μA cm^{-2}, $n = 4$, in the absence and presence of suramin, respectively, on the apical side). The P2Y antagonist Reactive Blue 2 (10 μM) was also ineffective (10 μM UTP, maximal I_{Cl} was $7{\cdot}7 \pm 0{\cdot}4$ and $6{\cdot}3 \pm 1{\cdot}0$ μA cm^{-2}, $n = 4$, in the absence and presence of Reactive Blue 2, respectively). Similar data were found with ATP (data not given).

Apical adenosine application also stimulated I_{Cl} (Fig. 8) with an EC_{50} of $5{\cdot}0 \pm 3{\cdot}6$ μM (Fig. 7). The presence of two types of purinoreceptors was confirmed when treating the cell monolayers with the adenoreceptor blocker theophylline. The stimulation of I_{Cl} by 100 μM UTP was not affected by the presence of 100 μM theophylline, while the adenosine response was totally abolished by this agent (I_{Cl} was $11{\cdot}8 \pm 3{\cdot}1$ and $0{\cdot}2 \pm 0{\cdot}1$ μA cm^{-2}, $n = 4$, in the absence and in the presence of theophylline, respectively).

Role of intracellular calcium in ATP-dependent Cl^- transport through the apical membranes

An intracellular calcium increase has been reported in many cell types upon external nucleotide application. In A6 cells, a transient increase in intracellular calcium was also observed after serosal or mucosal 300 μM ATP application (Fig. 9). The intracellular calcium peaks were of similar amplitudes (227 ± 27 and 226 ± 33 nM for serosal followed by apical ATP perfusion, $n = 7$) at 55 ± 7 s with serosal ATP application and 38 ± 10 s with an apical ATP application (difference not significant). The peak increase was followed by an intracellular calcium plateau of 145 ± 20 nM after apical ATP application and of 158 ± 26 nM with basolateral ATP application. A subsequent and significant decrease in intracellular calcium was observed after ATP washout (118 ± 14 and 130 ± 15 nM for serosal and mucosal washouts, respectively). These values were not significantly different from the initial control values.

In order to investigate whether an intracellular calcium increase could mimic the nucleotide stimulation of chloride transport, we tested two agents, ionomycin (5 μM) and thapsigargin (200 nM), previously reported to increase intracellular calcium when applied in A6 cells (Brochiero *et al.* 1997). Both thapsigargin (Fig. 10*A*) and ionomycin (Fig. 11*C*) transiently stimulated I_{Cl}. The maximal I_{Cl} values were $2{\cdot}2 \pm 0{\cdot}4$ μA cm^{-2} ($n = 8$) and $2{\cdot}1 \pm 0{\cdot}3$ μA cm^{-2} ($n = 3$) after ionomycin and thapsigargin application, respectively. The thapsigargin-stimulated current was subsequently blocked by DPC application (data not shown). Niflumic acid (100 μM) application blocked the ionomycin-stimulated current (the maximum stimulation was $3{\cdot}6 \pm 0{\cdot}3$ and $0{\cdot}1 \pm 0{\cdot}1$ μA cm^{-2} in the absence and presence of

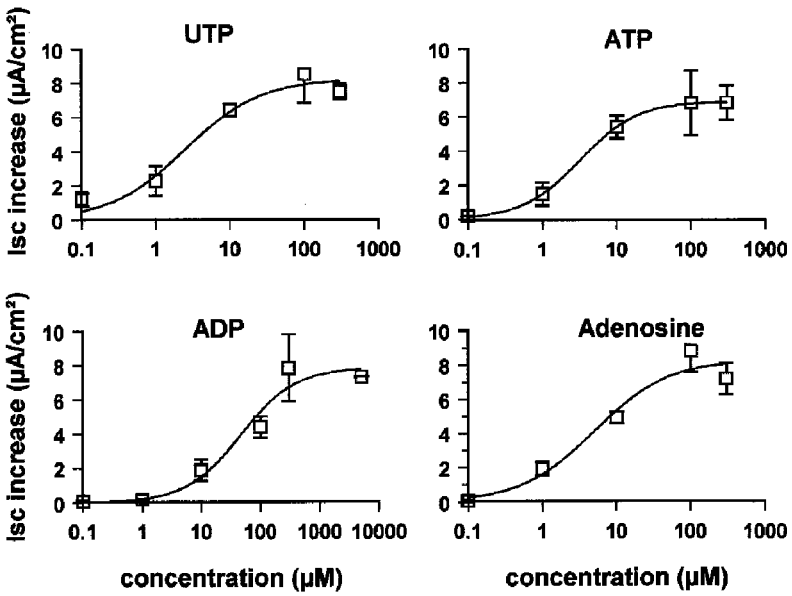

Figure 7. Concentration–response curves for UTP, ATP, ADP and adenosine

The nucleotides were added to the apical sides of cell monolayers. The curves represent the relation between maximal current increase (ordinate) and concentration (abscissa) of ATP ($n = 5$), UTP ($n = 5$), ADP ($n = 6$) and adenosine ($n = 5$). Means ± S.E.M. (vertical bars).

100 μM niflumic acid, respectively, $n = 3$). The UTP stimulation of the chloride transport was not suppressed when the cell monolayer was pretreated with ionomycin (Fig. 11*C*) or thapsigargin (Fig. 10*A*).

Conversely, the intracellular calcium chelator BAPTA-AM (40 μM), applied for 1 h before apical UTP (100 μM) application, largely inhibited the nucleotide response (maximal current after UTP in the absence and presence of BAPTA-AM was $7{\cdot}8 \pm 1{\cdot}0$ and $1{\cdot}1 \pm 0{\cdot}5$ μA cm^{-2}, respectively, $n = 4$).

Effects of Ca^{2+}–calmodulin inhibitors on chloride conductance

The above experiments indicate that application of apical nucleotides increases both $[Ca^{2+}]_i$ and the chloride conductance of the apical membranes and that the two agents (ionomycin and thapsigargin), known to increase

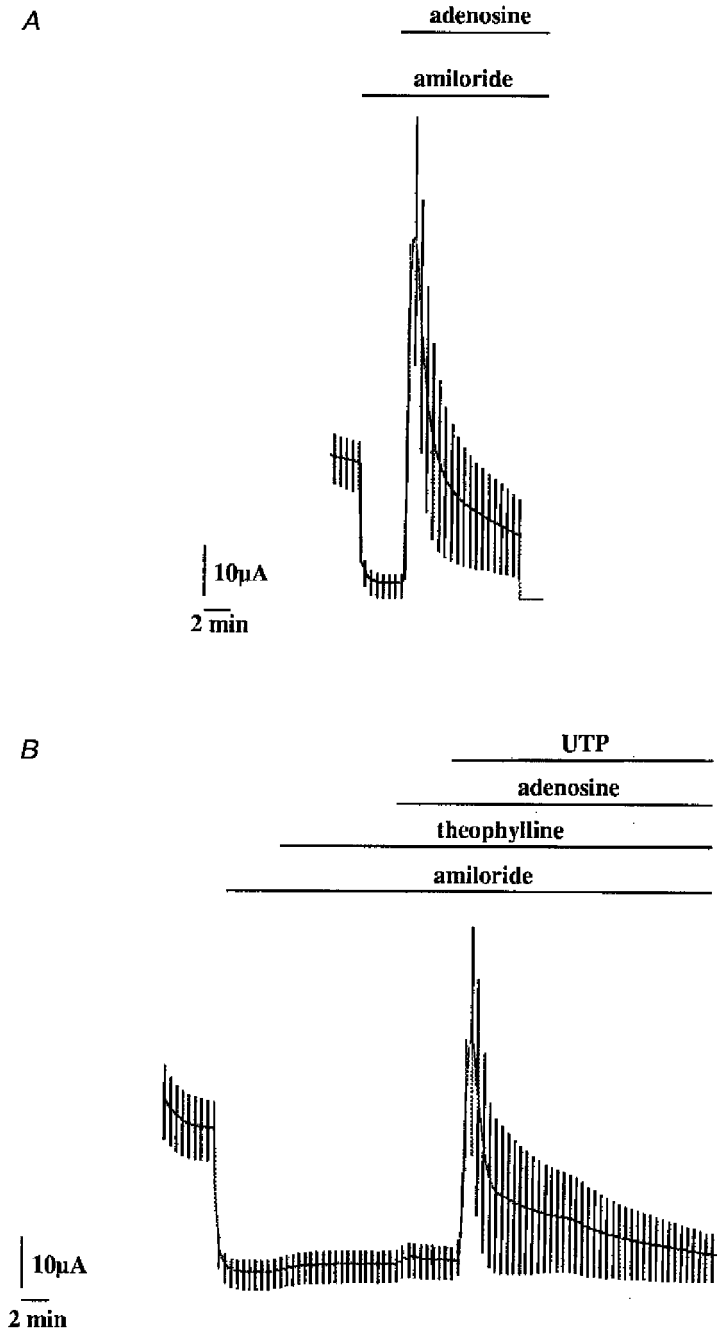

Figure 8. Effect of theophylline on the adenosine- or UTP-stimulated currents in A6 cell monolayers

Typical experiments showing the inhibitory effect of 100 μM theophylline (*B*) before 100 μM adenosine application (compared with the paired experiment in the absence of theophylline (*A*). Theophylline had no effect on the 100 μM UTP response. Theophylline, adenosine and UTP were all applied on the apical side of the cell monolayer.

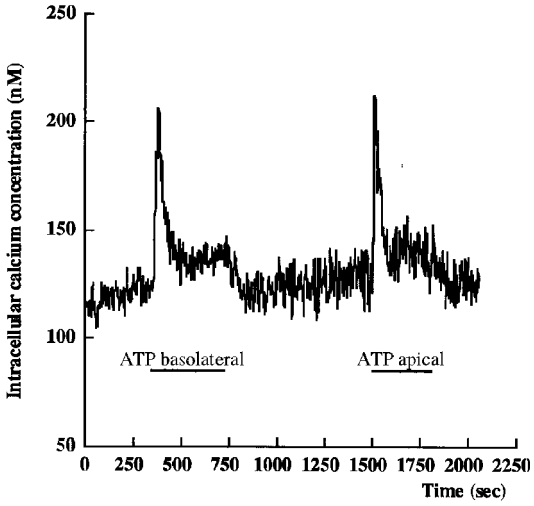

Figure 9. A transient increase in Ca_i^{2+} was observed after serosal or mucosal ATP application in A6 cell monolayers

A typical experiment is shown. The cell monolayer was continuously perfused.

$[Ca^{2+}]_i$ also lead to a stimulation of a chloride conductance. To investigate the role of Ca_i^{2+} as a mediator of the signalling pathway further, we tested the effects of chlorpromazin (50 μM), a Ca^{2+}–calmodulin inhibitor, on I_{Cl}. A representative experiment is given in Fig. 11. This agent applied for 10 min on the apical side of the monolayer had a marked inhibitory effect on I_{Cl} induced either by apical UTP or ionomycin application (Fig. 11). Maximal current after 300 μM UTP application in the absence and presence of chlorpromazin was $5{\cdot}6 \pm 0{\cdot}9$ and $1{\cdot}6 \pm 0{\cdot}3$ μA cm^{-2}, respectively ($n = 4$); maximal current after 5 μM ionomycin application in the absence and presence of chlorpromazin was $1{\cdot}7 \pm 0{\cdot}4$ and $0{\cdot}2 \pm 0{\cdot}2$ μA cm^{-2}, respectively, $n = 4$).

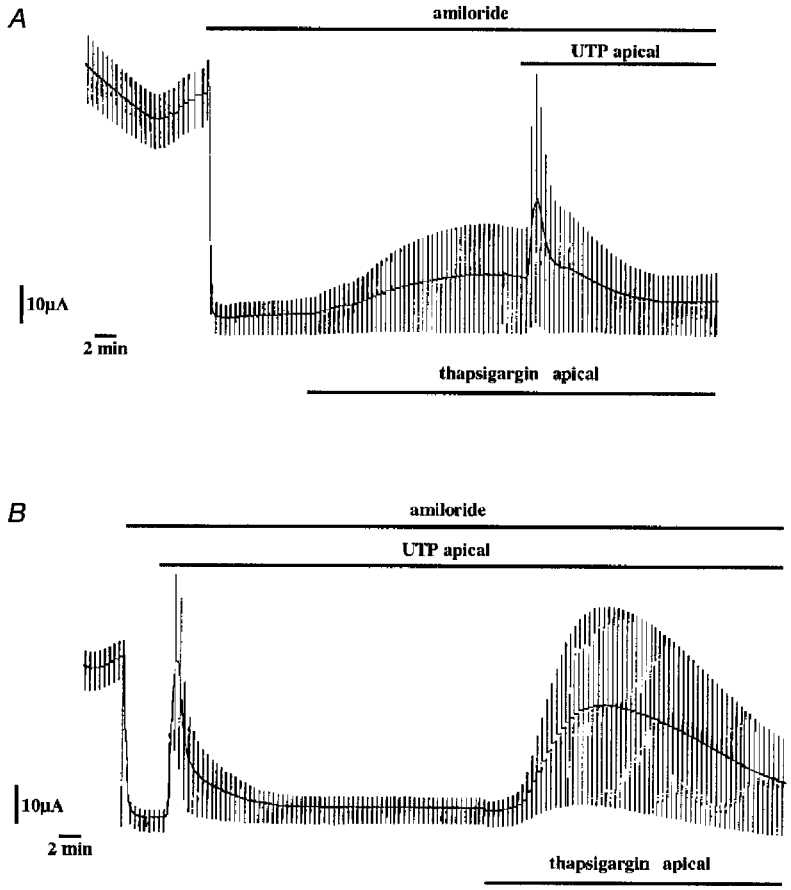

Figure 10. Effect of thapsigargin on the short-circuit current in A6 cell monolayers

Thapsigargin (200 nM) was added before (*A*) or after (*B*) UTP application. Note that the thapsigargin stimulation of I_{SC} was more progressive than the UTP response.

DISCUSSION

The distal nephron cell line A6 cells have been found to secrete Cl^- ions after serosal application of AVT (Yanase & Handler, 1986; Chalfant *et al.* 1993) or prostaglandin E_2 (Keeler & Wong, 1986). This Cl^- secretion results in the appearance of short-circuit current (I_{SC}) insensitive to amiloride which can be explained in term of the fluid secretion model first proposed by Silva *et al.* (1977) and recently reviewed by Begenish & Melvin (1998). In this model the chloride is secreted by a two-step process: a Na^+–K^+–$2Cl^-$ transporter (and/or a Cl^-–HCO_3^- exchanger) located on the basolateral membranes concentrates intracellular chloride above its electrochemical gradient (secondary active process) and chloride channels located on the apical membranes allow passive chloride diffusion once activated. The apical membrane is the rate-limiting pathway and therefore plays a determinant role in the rate of chloride secretion. Several chloride channels have been reported in A6 cell apical membranes (3 and 8 pS unit conductances) as revealed by patch-clamp experiments (Marunaka & Eaton, 1990*a*,*b*, 1993; Marunaka & Tohda, 1993).

The effects of external nucleotides on chloride secretion were investigated using various complementary approaches including relatively indirect techniques (such as I_{SC} measurements or aCl_i changes) and more direct ones (^{36}Cl effluxes through the apical membranes and patch-clamp experiments). These approaches lead to a single conclusion that extracellular ATP and UTP transiently stimulate the chloride secretion through the distal nephron cell line A6 by binding to purinergic receptors located on the apical membranes and the basolateral membranes. In this study we focused on the purinergic receptors of the apical membranes. A number of questions can be raised concerning the types of purinergic receptor and channel which are involved and the intracellular signalling pathway implicated.

Which purinergic receptors?

The interaction of purinergic agonists with specific receptors has been shown to induce a variety of biological responses in

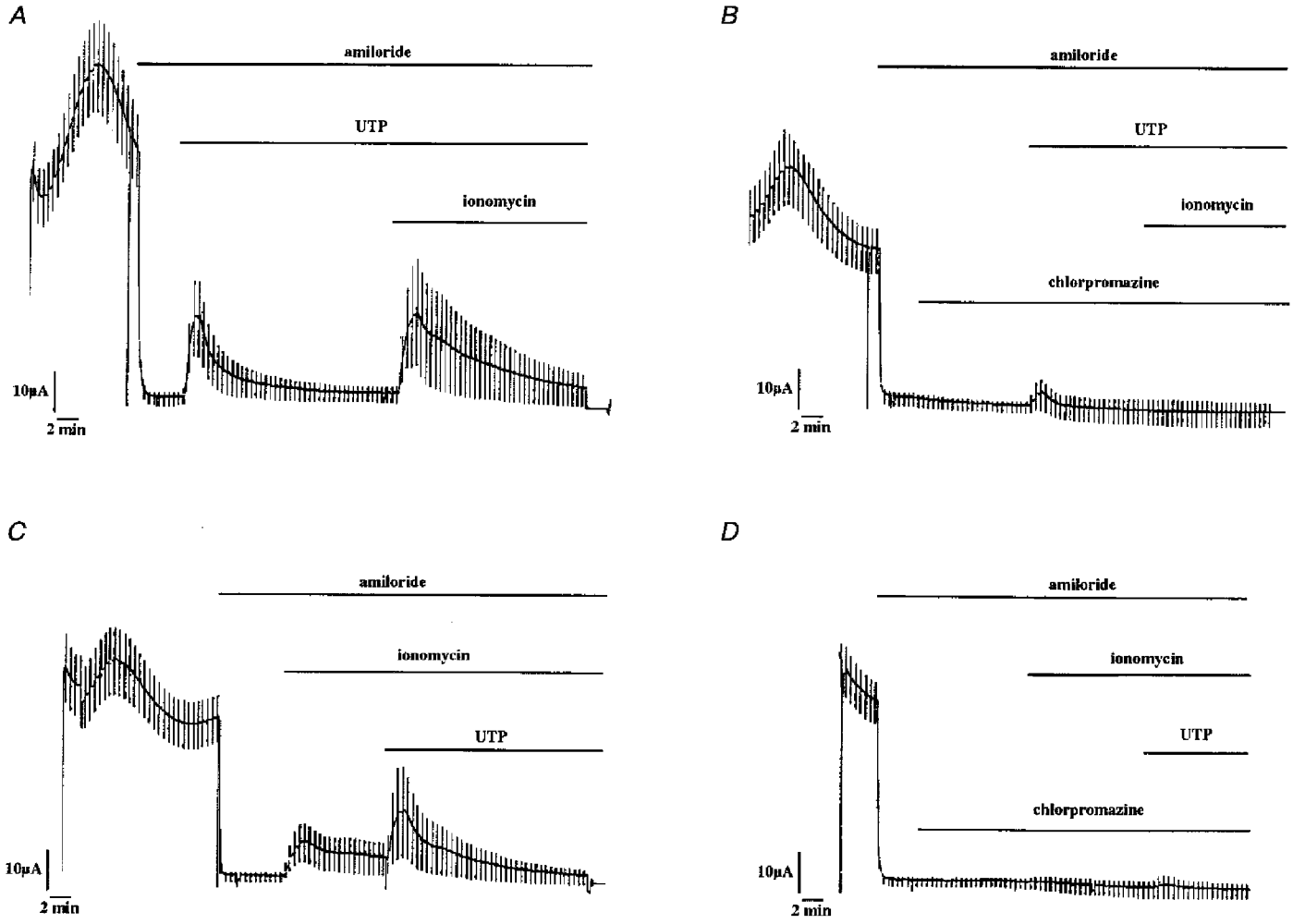

Figure 11. Effect of chlorpromazin on the UTP or ionomycin stimulated short-circuit current in A6 cell monolayers

Apical application of 50 μM chlorpromazin blocked UTP (300 μM)- or ionomycin (5 μM)-stimulated short-circuit currents. In *A* and *B*, UTP was applied before ionomycin whereas in *C* and *D* ionomycin was applied first.

a number of different cells. Based on their pharmacological and structural properties the receptors have been subdivided into P1 receptors, which are activated by adenosine, and P2 receptors which are activated by di- or triphosphate nucleotides (Burnstock, 1996; Barnard *et al.* 1997). At least four subtypes of adenosine receptor (A_1, A_{2A}, A_{2B} and A_3) have been identified on the basis of agonist and antagonist potency orders. The P1 receptors can activate phospholipase C and therefore elevate intracellular calcium concentration (for review see Müller & Stein, 1996). P2 receptors have been further subdivided into two classes: ligand gated ion channels (P2X receptors) and G protein-coupled receptors (P2Y receptors) (see Bhagwat & Williams, 1997; North & Barnard, 1997). Most P2Y receptors are coupled to phospholipase C, leading to an increase in the inositol 1,4,5-triphosphate ($InsP_3$) which therefore elevates intracellular calcium by mobilising intracellular stores.

Comparing the effects on the chloride secretion (I_{SC}), of agonists applied to the apical side of A6 cells, we determined the following order of potency: UTP = ATP > ADP > β,γ-methylene ATP = 2-methylthioATP. The trypanoside suramin (100 μM) had no effect on the UTP (or ATP)-stimulated current. The poor stimulatory effect of the agonist β,γ-methylene ATP, like the lack of effect of suramin application on the ATP- or UTP-stimulated current, suggests that P2X receptors are not involved in the I_{SC} response. This observation is reinforced by patch-clamp experiments since in the 'on' cell configuration, the increase in channel activity was observed in the membrane under the pipette which does not contain ATP, which therefore excludes a direct binding of the ligand to a receptor channel. Reactive Blue 2 (synonymous with Cibacron Blue), a non-competitive P2 receptor antagonist which does not discriminate between P2X and P2Y subtypes (for recent review, see Ralevic & Burnstock, 1998), also did not block I_{Cl}. Considering the I_{Cl} activation by the roughly equally potent UTP and ATP and the weak activation by ADP and other nucleoside diphosphate 2-methylthioATP and by β,γ-methylene ATP, it would appear that $P2Y_2$-like receptors located on the apical membranes of the A6 cells are implicated. In A6 cells grown on glass coverslips, Mori *et al.* (1996) deduced the presence of P2Y receptors and ATP activation of cation conductances. A similar study was made by Nilius *et al.* (1996) who demonstrated Ca^{2+} release and activation of K^+ and Cl^- currents in A6 cells by extracellular ATP, without determining the type of receptor involved. However, in neither study did the whole-cell voltage-clamp technique applied to non-polarised cells permit the localisation of the receptors or the stimulated channels of the membrane. In this context, the importance of the polarised phenotype to express UDP-sensitive receptors was recently demonstrated on equine cultured epithelia (Wilson *et al.* 1998).

Apical adenosine application was also found to stimulate I_{Cl}. The presence of another type of receptor, a P1 receptor, is therefore suggested and supported by the effect of the adenoreceptor blocker theophylline. Indeed, the stimulation of I_{SC} by UTP was not affected by the presence of theophylline, while the adenosine response was totally abolished by this agent, indicating the presence of two types of receptor.

Which chloride channels are implicated?

Two types of chloride channel, displaying single channel conductances of 3 and 8 pS, have been identified on the apical membranes of A6 cells grown on filters (references above). In the present study, the unitary single channel conductance found for apical chloride channels stimulated by ATP was 7·3 ± 0·6 pS, presenting a linear *I–V* relationship between −120 and +120 mV. This 7 pS Cl^- channel was found to be present under control conditions, but addition of ATP clearly induced the activation of one or more channels within a few minutes. The channel under discussion here shows several similarities to the 8 pS Cl^- channel described by Marunaka & Eaton (1990) and Shintani & Marunaka (1996). This channel also presented a linear *I–V* relationship, was found to be stimulated by Br-cAMP and was sensitive to NPPB.

The various drugs tested on the I_{Cl} or the ^{36}Cl effluxes furnished additional information on the pharmacology of the channel implicated in nucleotide-stimulated Cl^- secretion. ATP- or UTP-stimulated I_{Cl} was strongly blocked by DPC (200 μM) and niflumic acid (100 μM), moderately by DIDS (500 μM) and was insensitive to glibenclamide (100 μM). The inhibitory effect of DPC on Cl^- movements was documented by the inhibition of ^{36}Cl efflux noted across the apical membranes of ATP-stimulated monolayers. NPPB (50 μM) produced similar effects. It should be noted that the small residual ^{36}Cl efflux measured in non-stimulated conditions was also inhibited by NPPB and DPC. The presence of the cystic fibrosis transmembrane conductance regulator (CFTR) protein revealed by PCR (CFTR-mRNA detection) and by immunofluorescence techniques has been demonstrated in A6 cells (Price *et al.* 1996; Ling *et al.* 1997; Morris *et al.* 1998). In particular, Ling *et al.* (1997) found that in cell-attached patches, the 8 pS Cl^- channel activity was reduced in cells treated with CFTR antisense oligonucleotide as was the forskolin-activated amiloride-insensitive I_{SC}. It is therefore likely that the previously reported 8 pS Cl^- channel stimulated by an elevation of cAMP and the 7·3 pS Cl^- channel found in our study are in fact the same channel, but we cannot exclude the possibility of other channels being involved.

Nucleotide occupancy of P2Y receptors elevates $[Ca^{2+}]_i$ which in turn can increase epithelial chloride secretion (see Introduction). A6 cells follow this paradigm. The elevation of $[Ca^{2+}]_i$ reported in the present and previous studies (Nilius *et al.* 1995; Mori *et al.* 1996; Brochiero *et al.* 1997) was associated with the stimulation of a chloride current (see Introduction). Thus, it is probable that $[Ca^{2+}]_i$ plays a major role in the stimulation of the apical chloride channels. This interpretation is supported by our findings that pre-treatment of the monolayer with BAPTA-AM, a $[Ca^{2+}]_i$

chelator, prevented the UTP-stimulated I_{Cl} and the adenosine-stimulated I_{Cl} (data not shown). The marked inhibitory effect of chlorpromazine on I_{Cl} induced either by apical UTP application or by ionomycin application also points to a major role of $[Ca^{2+}]_i$ in the signalling pathway of A6 cells. In addition, it indicates that a Ca_i^{2+}–calmodulin protein kinase may be involved in the response. It is relevant that in normal and cystic fibrosis airway epithelial cells, Ca^{2+} activation of Cl^- channels was found to be mediated by a multifunctional Ca^{2+}–calmodulin-dependent kinase (Wagner *et al.* 1991). A similar finding was reported for cystic fibrosis pancreatic epithelial cells (Chao *et al.* 1995). Alternatively (or in addition), the Ca^{2+} activation of Cl^- channels may be a secondary event that follows activation of calcium-sensitive K^+ channels located in the basolateral membranes. The consequent hyperpolarisation is thought to increase the driving force for Cl^- exit through the apical membranes. This mechanism has been proposed for T84 cells (Dharmsathaphorn & Pandol, 1986; Dharmsathaphorn *et al.* 1989; Dho *et al.* 1992). An additional indirect role for calcium would be its involvment in the trafficking of apical chloride channels. In A6 cells, such a recruitment of cytoplasmic CFTR to the apical cell surface upon AVT stimulation was recently demonstrated by immunocytochemical studies; furthermore, microtubule disruption inhibited the AVT-stimulated Cl^- secretion (Morris *et al.* 1998). On the other hand, the increase in $[Ca^{2+}]_i$ could act directly on the Cl^- channel. The inhibitory effect of niflumic acid on the nucleotide- and on ionomycin-stimulated chloride currents argues for the presence of calcium-stimulated chloride channels, since this drug has been described as a potent blocker of Ca^{2+}-activated I_{Cl} (Ackerman *et al.* 1994).

The precise relationships between the $[Ca^{2+}]_i$ increase observed upon nucleotide application and the stimulation of chloride secretion in A6 cells remain to be determined.

In conclusion, the localisation of adenosine purinoreceptors and pyrimidine nucleotides on the apical surface of epithelial cells suggests that these nucleotides could act as autocrine or paracrine modulators of Cl^- secretion in the renal cells as found in other epithelia (Mitchell *et al.* 1998; Taylor *et al.* 1999).

Ackerman, M. J., Wickman, K. D. & Clapham, D. E. (1994). Hypotonicity activates a native chloride current in *Xenopus* oocytes. *Journal of General Physiology* **103**, 153–179.

Barnard, E. A., Simon, J. & Webb, T. E. (1997). Nucleotide receptors in the nervous system. An abundant component using diverse transduction mechanisms. *Review of Molecular Neurobiology* **15**, 103–129.

Begenisich, T. & Melvin, J. E. (1998). Regulation of chloride channels in epithelia. *Journal of Membrane Biology* **163**, 77–85.

Bhagwat, S. S. & Williams, M. (1997). Purine and pyrimidine receptors: emerging superfamilies of G-protein-coupled and ligand-gated-ion channel receptors. *European Journal of Medical Chemistry* **32**, 183–193.

Brochiero, E., Banderali, U., Lindenthal, S., Raschi, C. & Ehrenfeld, J. (1995*a*). Basolateral membrane chloride permeability of A6 cells: implication in cell volume regulation. *Pflügers Archiv* **431**, 32–46.

Brochiero, E., Raschi, C. & Ehrenfeld, J. (1995*b*). Na/Ca exchange in the basolateral membrane of the A6 monolayer: role in Ca_i homeostasis. *Pflügers Archiv* **430**, 105–114.

Brochiero, E., Raschi, C. & Ehrenfeld, J. (1997). Characterization of the Ca^{2+} membrane permeability of serial A6 cells upon different osmotic conditions. *Kidney and Blood Pressure Research* **20**, 381–390.

Burnstock, G. (1996). P2 purinoceptors: historical perspective and classification. *Ciba Foundation Symposium*, vol. 198, pp. 1–28; Discussion 29–34. Review.

Chalfant, M. L., Coupaye-Gerard, B. & Kleyman, T. (1993). Distinct regulation of Na^+ absorption and Cl^- secretion by arginine vasopressin in the amphibian cell line A6. *American Journal of Physiology* **264**, C1480–1488.

Chao, A. C., Kouyama, K., Heist, E. K., Dong, Y. J. & Gardner, P. (1995). Calcium- and CaMKII-dependent chloride secretion induced by the microsomal Ca(2+)-ATPase inhibitor 2,5-di-(tert-butyl)-1,4-hydroquinone in cystic fibrosis pancreatic epithelial cells. *Journal of Clinical Investigation* **96**, 1794–1801.

Clarke, L. L. & Boucher, R. C. (1992). Chloride secretory response to extracellular ATP in normal and cystic fibrosis nasal epithelia. *American Journal of Physiology* **263**, C348–356.

Crowe, W. E., Ehrenfeld, J., Brochiero, E. & Wills, N. K. (1995). Apical membrane sodium and chloride entry during osmotic swelling of renal (A6) epithelial cells. *Journal of Membrane Biology* **144**, 81–91.

Denicourt, N., Cai, S., Garneau, L., Brunette, M. G. & Sauvé, R. (1996). Evidence from incorporation experiments for an anionic channel of small conductance at the apical membrane of the rabbit distal tubule. *Biochimica et Biophysica Acta* **1285**, 155–166.

Dharmsathaphorn, K. J., Cohn, J. & Beuerlein, G. (1989). Multiple calcium-mediated effector mechanisms regulate chloride secretory responses in T84-cells. *American Journal of Physiology* **256**, C1224–1230.

Dharmsathaphorn, K. J. & Pandol, S. J. (1986). Mechanism of chloride secretion induced by carbachol in a colonic epithelial cell line. *Journal of Clinical Investigation* **77**, 348–354.

Dho, S., Stewart, K. & Foskett, J. K. (1992). Purinergic receptor activation of Cl^- secretion in T84 cells. *American Journal of Physiology* **262**, C67–74.

Ehrenfeld, J., Raschi, C. & Brochiero, E. (1994). Basolateral potassium membrane permeability of A6 cells and cell volume regulation. *Journal of Membrane Biology* **138**, 181–195.

Fan, P. Y., Haas, M. & Middleton, J. P. (1992). Identification of a regulated Na/K/Cl cotransport system in a distal nephron cell line. *Biochimica et Biophysica Acta* **1111**, 75–80.

Grynkiewicz, G., Poenie, M. & Tsien, R. Y. (1985). A new generation of Ca^{2+} indicators with greatly impoved fluorescence properties. *Journal of Cell Biology* **6**, 3440–3450.

Handler, J. S., Steele, R. E., Sahib, M. K., Wade, J. B., Preston, A. S., Lawson, N. S. L. & Johnson, J. P. (1979). Toad urinary bladder epithelial cells in culture: Maintenance of epithelial structure, sodium transport, and response to hormones. *Proceedings of the National Academy of Sciences of the USA* **76**, 4151–4155.

Horn, R. (1991). Estimating the number of channels in patch recordings. *Biophysical Journal* **60**, 433–439.

Keeler, R. & Wong, N. L. M. (1986). Evidence that prostaglandin E_2 stimulates chloride secretion in cultured A6 serial epithelial cells. *American Journal of Physiology* **250**, F511–515.

Ling, B. N., Zuckerman, J. B., Lin, C., Harte, B. J., McNulty, K. A., Smith, P. R., Gomez, L. M., Worrell, R. T., Eaton, D. C. & Kleyman, T. R. (1997). Expression of the cystic fibrosis phenotype in a renal amphibian epithelial cell line. *Journal of Biological Chemistry* **272**, 594–600.

Marunaka, Y. (1993). Modification of Ca^{2+}-sensitivity of Ca^{2+}-activated Cl^- channel by vasopressin and cholera toxin. *Japanese Journal of Physiology* **43**, 553–560.

Marunaka, Y. & Eaton, D. C. (1990*a*). Chloride channels in the apical membrane of a distal nephron A6 cell line. *American Journal of Physiology* **258**, C352–368.

Marunaka, Y. & Eaton, D. C. (1990*b*). Effects of insulin and phosphatase on a Ca^{2+} dependent Cl^- channel in a disatal nephron cell line (A6). *Journal of General Physiology* **95**, 773–789.

Marunaka, Y. & Tohda, H. (1993). Effects of vasopressin on single Cl^- channels in the apical membrane of distal nephron cells (A6). *Biochimica et Biophysica Acta* **1153**, 105–110.

Mori, M., Nishizaki, T., Kawahara, K. & Okada, Y. (1996). ATP-activated cation conductance in a *Xenopus* renal epithelial cell line. *Journal of Physiology* **491**, 281–290.

Morris, R. G., Tousson, A., Benos, D. J. & Schafer, J. A. (1998). Microtubule disruption inhibits AVT-stimulated Cl^- secretion but not Na^+ reabsorption in A6 cells. *American Journal of Physiology* **274**, F300–314.

Middleton, J. P., Mangen, A. W., Basavappa, S. & Fitz, G. (1993). Nucleotide receptors regulate membrane ion transport in renal epithelial cells. *American Journal of Physiology* **264**, F867–873.

Mitchell, C. H., Carre, D. A., McGlinn, A. M., Stone, R. A. & Civan, M. M. (1998). A release mechanism for stored ATP in ocular ciliary epithelial cells. *Proceedings of the National Academy of Sciences of the USA* **95**, 7174–7178.

Müller, C. E. & Stein, B. (1996). Adenosine receptor antagonists: structures and potential therapeutic applications. *Current Pharmaceutical design* **2**, 501–530.

Nilius, B., Sherer, J., Heinke, S. & Droogmans, G. (1995). Ca^{2+} release and activation of K^+ and Cl^- currents by extracellular ATP in distal eithelia cells. *American Journal of Physiology* **269**, C376–384.

North, R. A. & Barnard, E. A. (1997). Nucleotide receptors. *Current Opinion in Neurobiology* **7**, 346–357.

Perkins, F. M. & Handler, J. S. (1981). Transport properties of toad kidney epithelium in culture. *American Journal of Physiology* **241**, C154–159.

Price, M. P., Ishihara, H., Sheppard, D. N. & Welsh, M. J. (1996). Function of *Xenopus* cystic fibrosis transmembrane regulator (CFTR) Cl channels and use of human-Xenopus chimeras to investigate the pore properties of CFTR. *Journal of Biological Chemistry* **271**, 25184–25191.

Rabe, A., Disser, J. & Fromter, E. (1995). Cl^- channel inhibition by glibenclamide is not specific for the CFTR-type Cl^- channel. *Pflügers Archiv* **429**, 659–662.

Ralevic, V. & Burnstock, G. (1998). Receptors for purines and pyrimidines. *Pramacological Reviews* **50**, 313–492.

Rugolo, M., Mastrocola, T., Whörle, C., Rasola, A., Gruenert, D. C., Romeo, G. & Galietta, L. J. V. (1993). ATP and A1 adenosine receptors agonists mobilize intracellular calcium and activate K^+ and Cl^- currents in normal and cystic fibrosis airway epithelial cells. *Journal of Biological Chemistry* **268**, 24779–24784.

Sariban-Sohraby, S., Burg, M. B. & Turner, R. J. (1983). Apical sodium uptake in the toad kidney epithelial cell line A6. *American Journal of Physiology* **245**, C167–171.

Sheppard, D. N. & Welsh, M. J. (1993). Inhibition of the cystic fibrosis transmembrane conductance regulator by ATP-sensitive K^+ channel regulators. *Annals of the New York Academy of Sciences* **707**, 275–284.

Shintani, Y. & Marunaka, Y. (1996). Regulation of chloride channel trafficking by cyclic AMP via protein kinase A-independent pathway in A6 renal epithelial cells. *Biochemical and Biophysical Research Communication* **223**, 234–239.

Silva, P. J., Staff, J., Fiels, J., Fine, L., Forest, J. N. & Epstein, F. H. (1977). Mechanism of active chloride secretion by shark rectal gland: role of Na-K-ATPase in chloride transport. *American Journal of Physiology* **233**, F298–306.

Taylor, A. L., Kudlow, B. A., Marrs, K. L., Gruenert, D. C., Guggino, W. B. & Schwiebert, E. M. (1999). Bioluminescence detection of ATP release mechanisms in epithelia. *American Journal of Physiology* **275**, C1391–406

Verrey, F. (1994). Antidiuretic hormone action in A6 cells: Effect on apical Cl and Na conductances and synergism with aldosterone for NaCl reabsorption. *Journal of Membrane Biology* **138**, 65–76.

Verrey, F., Schaerer, E., Zoerkler, P., Paccolat, M. P., Geering, K., Kraehenbuhl, J. P. & Rossier, B. C. (1987). Regulation by aldosterone of Na^+,K^+-ATPase mRNAm, protein synthesis, and sodium transport in cultured kidney cells. *Journal of Cell Biology* **104**, 1231–1237.

Wagner, J. A., Cozens, A. L., Schulman, H., Gruenert, D. C., Stryer, L. & Gardner, P. (1991). Activation of chloride channels in normal and cystic fibrosis airway epithelia cells by multifunctional calcium/calmodulin-dependent protein kinase. *Nature* **349**, 193–196.

Wilson, S. M., Law, V. W. Y., Pediani, J. D., Allen, E. A., Wilson, G., Khan, Z. E. & Ko, W. H. (1998). Nucleotide-evoked calcium signals and anion secretion in equine cultured epithelia that express apical P2Y2 receptors and pyrimidine nucleotide receptors. *British Journal of Pharmacology* **124**, 832–838.

Yanase, M. & Handler, J. S. (1986). Adenosine 3′,5′-cyclic monophosphate stimulates chloride secretion in A6 epithelia. *American Journal of Physiology* **251**, C810–814.

Zegarra-Moran, O., Romeo, G. & Galietta, L. J. V. (1995). Regulation of transepithelial ion transport by two different purinoreceptors in the apical membrane of canine kidney (MDCK) cells. *British Journal of Pharmacology* **114**, 1052–1056.

Acknowledgements

The authors would like to thank Dr M. Civan for reading the manuscript. This work was supported by the CNRS, the MENSRT and the CEA.

Corresponding author

J. Ehrenfeld: Laboratoire de Physiologie des membranes cellulaire (Laboratoire Jean Maetz), Université de Nice Sophia Antipolis, ERS 1253 (CNRS), BP 68, Villefranche-sur-mer 06238, France.

Email: ehrenfeld@ccrv.obs-vlfr.fr